JOURNAL OF SOLID STATE CHEMISTRY 61, 212–222 (1986)

Observation of the Verwey Transition in Fe_3O_4 by High-Resolution Electron Microscopy

NOBUO OTSUKA AND HIROSHI SATO

School of Materials Engineering, Purdue University, West Lafayette, Indiana 47907

Received February 19, 1985; in revised form June 26, 1985

High resolution electron microscopy (HREM) of Fe_3O_4 has been carried out at temperatures near the Verwey transition (~120 K) with a point resolution of 3 Å. Lattice fringes of both the high- and the low-temperature phases have been observed at these temperatures. The crystal symmetry of the low-temperature phase indicated by the lattice images is consistent with the result obtained by earlier diffraction studies. A series of lattice images showing the transition from the low-temperature phase (to the high-temperature phase) has been obtained. The transformation to the high-temperature phase occurs through the penetration of the high-temperature phase into areas of the low-temperature phase. A quick motion of domain boundaries in the low-temperature phase, which is consistent with almost instantaneous rearrangements of charge ordering, has been observed. The possibility of determining the ordered arrangement of Fe^{2+} and Fe^{3+} ions directly by HREM is discussed.

Introduction

On cooling, Fe_3O_4 has been known to undergo a first-order phase transition (the Verwey transition) at around 120 K (*1–3*). The transition is accompanied by a sharp drop in the electrical conductivity and a slight distortion of the crystal lattice. The origin of the transition has been ascribed to the ordering of Fe^{2+} and Fe^{3+} ions on the octahedral interstitial sites (B sites) in the spinel lattice (*3*). Since the ordering of Fe^{2+} and Fe^{3+} can be accomplished through a redistribution of electrons, it is called charge ordering. The clarification of the charge ordering phenomena or of their possible differences from chemical ordering phenomena has attracted a great deal of attention.

A large number of studies have been carried out to determine the ordered structure in the low-temperature phase. It has been found from the observation of superstructure reflections by electron and neutron diffraction (*4, 5*) that the ordered structure is more complicated than the original model proposed by Verwey (*3*). Single-crystal X-ray diffraction studies have shown that the ordered structure is base-centered monoclinic with cell parameters, $a = 11.888$ Å, $b = 11.847$ Å, $c = 16.773$ Å, and $\beta = 89.76°$ at 84 K (*6, 7*).[1] The axes a, b, and c correspond to the $[110]_c$, the $[1\bar{1}0]_c$, and the

[1] Studies of the magnetoelectric effect indicate a further minor deviation from the monoclinic symmetry (*8–10*). This distortion, however, has not been detected by diffraction studies, and for practical purposes, this minor distortion can be neglected.

0022-4596/86 $3.00

$[001]_c$ axes of the high-temperature cubic spinel lattice.[2] (The relation between the orientation of the cubic lattice and the monoclinic lattice is shown in Fig. 1.) Atomic displacements associated with the transition have been analyzed in detail by recent diffraction studies (*11–13*). Because of the small difference in the scattering power of Fe^{2+} and Fe^{3+} ions, however, these diffraction studies could not explicitly determine the ordered arrangement of Fe^{2+} and Fe^{3+} ions. In other words, based on diffraction studies, it has not yet been clearly established that the transition is due to the charge ordering.

Mössbauer spectroscopy (*14–19*) and NMR (*15, 20–23*) have been applied to studies of the ordered arrangement of Fe^{2+} and Fe^{3+} ions in the low-temperature phase. The results, however, are found to be too complicated to determine the ordered arrangement uniquely. Furthermore, the symmetry of ordered structure suggested by these studies often contradicts with that obtained by diffraction studies: these results indicate that the symmetry of the crystal is even lower than base-centered monoclinic. Such complicated situations in determining the ordered arrangements have been major obstacles for understanding the nature of this transition. Some attempts have been made to reconcile the controversies with respect to the arrangement of Fe^{2+} and Fe^{3+} ions by introducing models such as partial charge ordering (*24*) and intrinsic antiphase microscopic domains (*25*), but such possibilities have not been confirmed experimentally.

As demonstrated by many recent studies, high-resolution electron microscopy (HREM) has now been established as one of the most powerful techniques for studying structures directly (*26*). Since HREM can reveal atomic structures directly in the real space, it can be very effective for clarifying ambiguities in structures. We have developed a HREM technique at temperatures near liquid nitrogen with a point resolution of 3 Å (the same resolution as that obtainable at ambient temperatures of the microscope used) and applied this technique to the observation. Lattice fringes of the low-temperature phase were thus clearly observed for the first time.

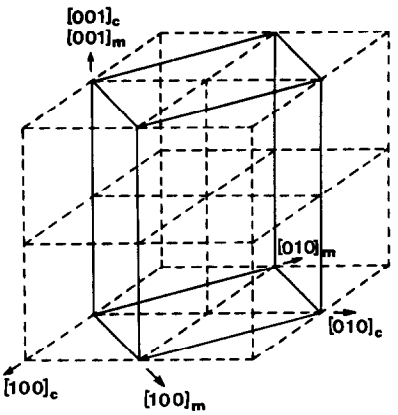

FIG. 1. The relation between the orientation of the high-temperature cubic lattice and the low-temperature monoclinic lattice of Fe_3O_4.

Experimental Procedures

Single crystals of Fe_3O_4 were grown by the skull melting technique. Compositions of the crystals were kept close to that of the stoichiometric by controlling the oxygen partial pressure during the growth. The detailed procedures were described in an earlier report (*27, 28*). Crystals were cut into thin slices and chemically etched with HCl.

A JEM 200CX electron microscope with a side-entry goniometer was used for the observation. The instrument has a resolution limit of 3.0 Å at the Schertzer defocus (−977Å) under axial illumination. A low-temperature specimen holder with a liquid nitrogen reservoir was used. The liquid nitrogen reservoir is connected to the speci-

[2] In this paper hkl_c and hkl_m are used for indices based on the cubic and monoclinic lattices, respectively.

men supporter with a copper conduction rod. To avoid mechanical vibrations from the bubbling of the coolant, liquid nitrogen was removed from the reservoir immediately before recording images. Because of a large heat capacity of the holder, several pictures can be taken before the drift of image due to the change of temperature becomes appreciable. By this method, the same resolution as that of ambient temperature could be obtained. Since the specimen holder was capable of only single tilting, the orientation of crystals is adjusted manually outside the microscope and examined each time by observing electron diffraction patterns during this experiment.

Results and Discussion

Figures 2a and b are a high-resolution image and a corresponding diffraction pattern taken from a thin area of a Fe_3O_4 single crystal at 100 K. The image was obtained under axial illumination with the beam direction $[211]_c$ at nearly the Schertzer defocus. The image shows the coexistence of the low-temperature and the high-temperature phases. The thin area along the edge exhibits one-dimensional lattice fringes whose spacing is 4.7 Å. The spacing coincides with the interplanar spacing of the $(111)_c$ lattice planes of the high-temperature cubic phase. On the other hand, the thick area, which remains in the low-temperature phase, shows two-dimensional lattice fringes both of which have a spacing of 7.4 Å. These lattice fringes are due to the 111_m and the $11\bar{1}_m$ superstructure reflections of the low-temperature monoclinic phase. The presence of the high-temperature phase near the edge indicates an inhomogeneous temperature distribution in the specimen due to heating by electron beam which is not dissipated due to the poor thermal conductivity of the thin part of the specimen. In the present observation, the high-temperature phase is always found along the edges of specimens, and areas of the high temperature phase gradually spread into thick parts of crystals during the observations. No transitional structure has been observed in the boundary areas of the low-temperature and the high-temperature phases as seen in Fig. 2a. This observation is consistent with recent studies (*25, 29, 30*) which show that for nearly stoichiometric magnetite the transition occurs in one sharp discontinuous change rather than multistage processes suggested by earlier studies (*1, 31*).

Figure 2c is a magnified image of the area of the low-temperature phase seen in Fig. 2a. Because the intensities of superstructure reflections are low and the exposure time in the present method is limited, the contrast of lattice fringes is extremely low. The image, however, clearly shows a regular and uniform fringe pattern. No sign is seen of extended defects such as microscopic antiphase domains; these have been suggested by some researchers (*25*) in order to reconcile contradictions in the reported crystal symmetry as determined by diffraction studies and by some physical measurements (*23*). The observation of regular lattice fringes due to superstructure reflections also indicates that the ordered arrangement of Fe^{2+} and Fe^{3+} ions is of static nature. In other words, the charge ordering is spatially fixed just as the chemical ordering and continuous spacial drift motion of the structure with time is not expected. Figure 3a is a HREM image of the low-temperature phase with the beam direction along $[001]_m$ (with a corresponding diffraction pattern (Fig. 3b)). Although the contrast of the lattice fringes is very low, the image shows clearly a regular arrangement of lattice fringes due to 110_m and $1\bar{1}0_m$ superstructure reflections. (Lattice images of the low-temperature phase of various beam orientations such as $[221]_m$ and $[110]_m$ were also taken.) All observed HREM images of the low-temperature phase thus obtained

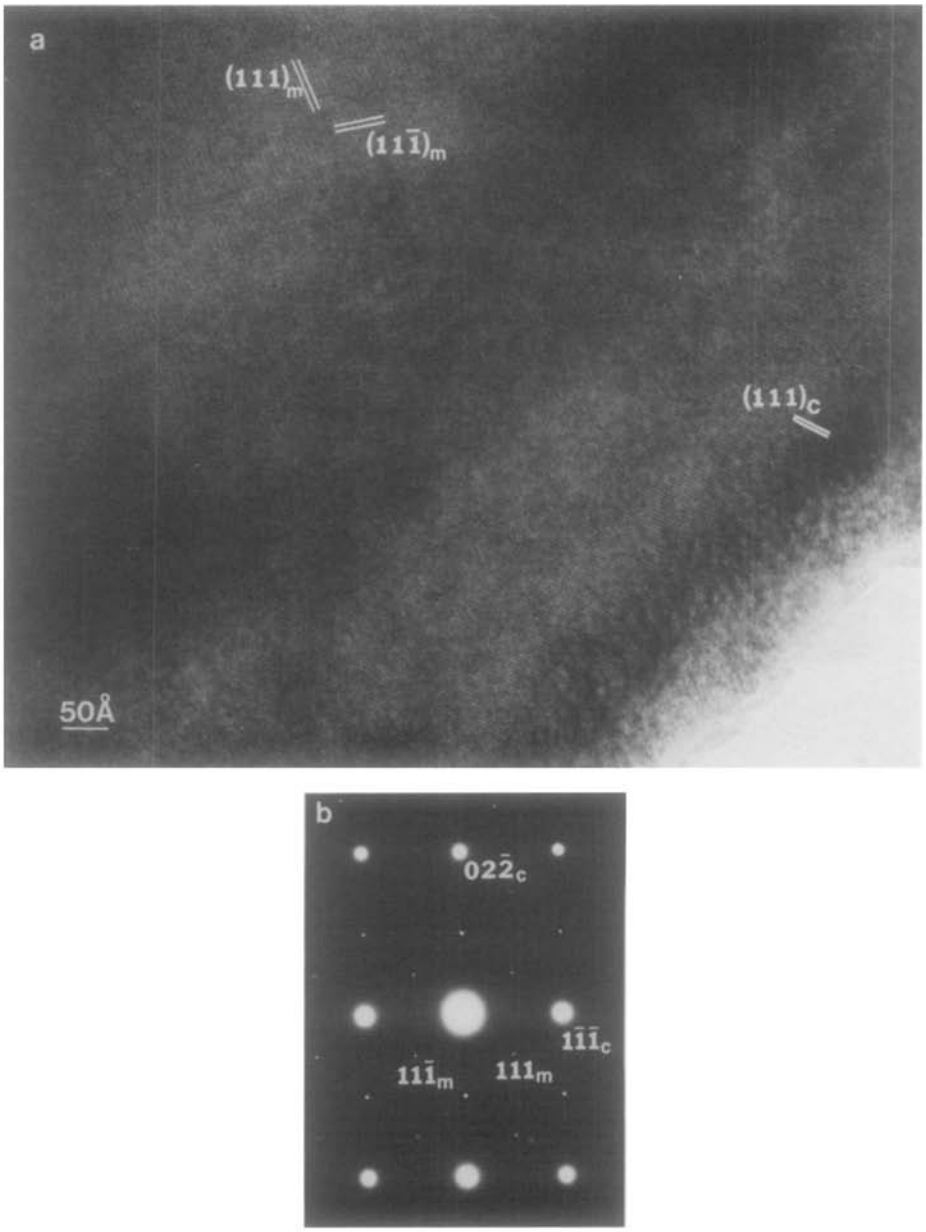

FIG. 2a. A high-resolution image taken from a Fe_3O_4 single crystal at 100 K. The beam direction is parallel to the $[\bar{2}11]$ axis of the cubic spinel lattice. Fig. 2b. A corresponding electron diffraction pattern. Weak spots are superstructure reflections due to the ordering of Fe^{2+} and Fe^{3+} ions.

have been carefully examined, but no lattice fringes having the spacing larger than those expected from the base-centered monoclinic lattice proposed by diffraction studies and thus indicating a lower symmetry have been found. Therefore, it can be

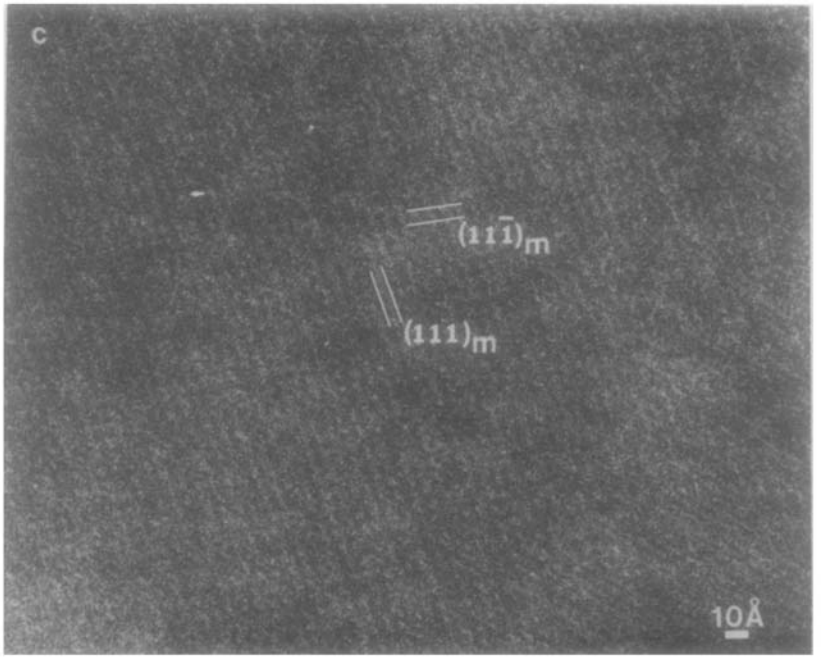

FIG. 2c. A magnified image of the area of the low-temperature phase seen in (a).

concluded that the crystal symmetry of the low-temperature phase is base-centered monoclinic as observed by diffraction studies, even on the microscopic scale as revealed by HREM.

As described earlier, areas of the low-temperature phase were found to gradually transform to the high-temperature phase due to the heating by electron beam. This gives us an opportunity of directly observing the transition through lattice imaging. The images in Figs. 4a–d were recorded from the same area successively at roughly 10-sec intervals. The beam direction of these images is parallel to the $[100]_c$ axis. The area of the low-temperature phase shows the $(001)_m$ lattice fringes whose spacing is 16 Å, while the area of the high-temperature phase does not show any lattice fringe. This situation arises because the largest spacing of lattice planes of the high-temperature phase belonging to the $[100]_c$ zone axis is only 2.9 Å, which is smaller than the resolution limit of the instrument. From Figs. 4a to d, it is seen that the area of the low-temperature phase gradually decreases as observed through the disappearance of the $(001)_m$ lattice fringes. An interesting feature is that the high-temperature phase first penetrates into the area of the low-temperature phase as a narrow band as indicated by an arrow in (b), and then gradually spreads (c), leaving an island of the low-temperature phase (indicated by an arrow) (d), which eventually disappears. This process may indicate a characteristic feature of the change from the ordered arrangement of Fe^{2+} and Fe^{3+} ions to the disordered one in this transition where no major atomic motion is expected.

Electrical and magnetic properties of the low-temperature phase represent the response of electrons which are involved in the charge ordering to applied fields; an understanding of these properties is the most important aspect in the study of the transi-

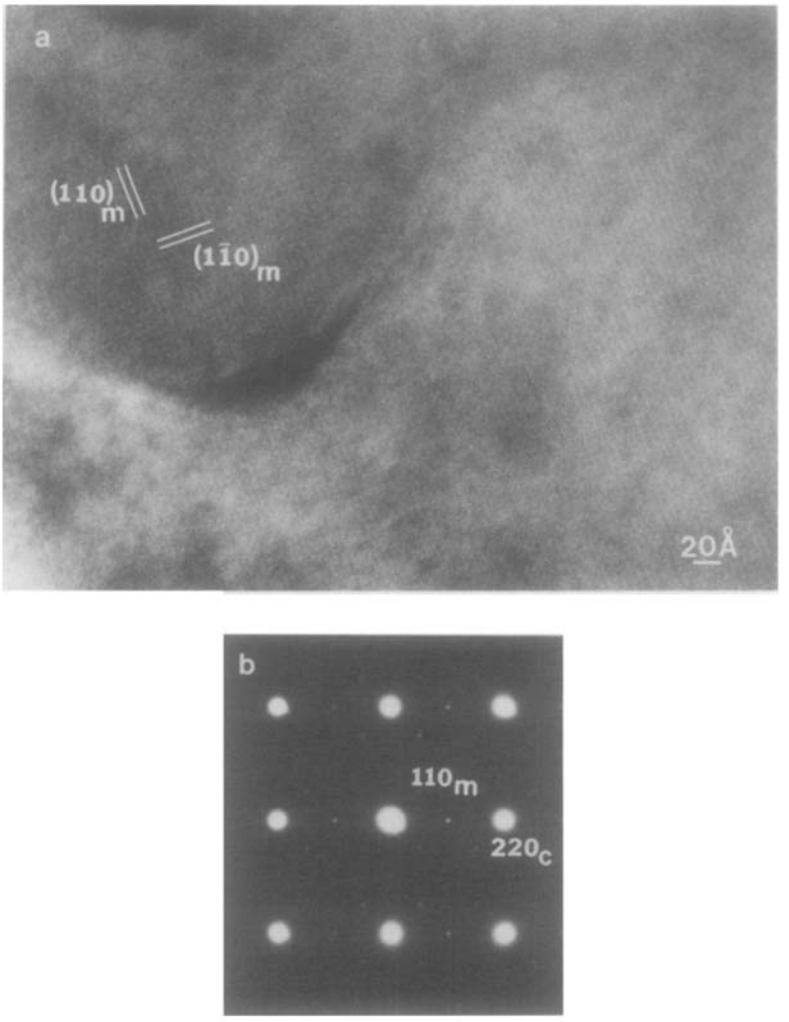

FIG. 3. A high-resolution image (a) and electron diffraction pattern (b) taken from a Fe_3O_4 single crystal at 100 K. The beam direction is parallel to the $[001]_m$ axis of the monoclinic lattice of the low-temperature phase.

tion (*32–36*). In addition, in the low-temperature phase, single crystals at high temperatures can be broken up into three kinds of twin domains (two with approximately the same *c* axis and one with different directions of the *c* axis); the physical properties sensitively depend on the distribution of such domains. The relative ease of the motion of such domain boundaries under external forces such as stress and magnetic field (and, hence, the difference in the distribution of these domains under different experimental conditions) can cause considerable complications in the interpretation of measured results. During the observation, dynamical behavior such as a quick motion of domain boundaries, possibly due to an inhomogeneous heating by electron beam, could be observed. Figure 5a shows a HREM image of a domain boundary (indi-

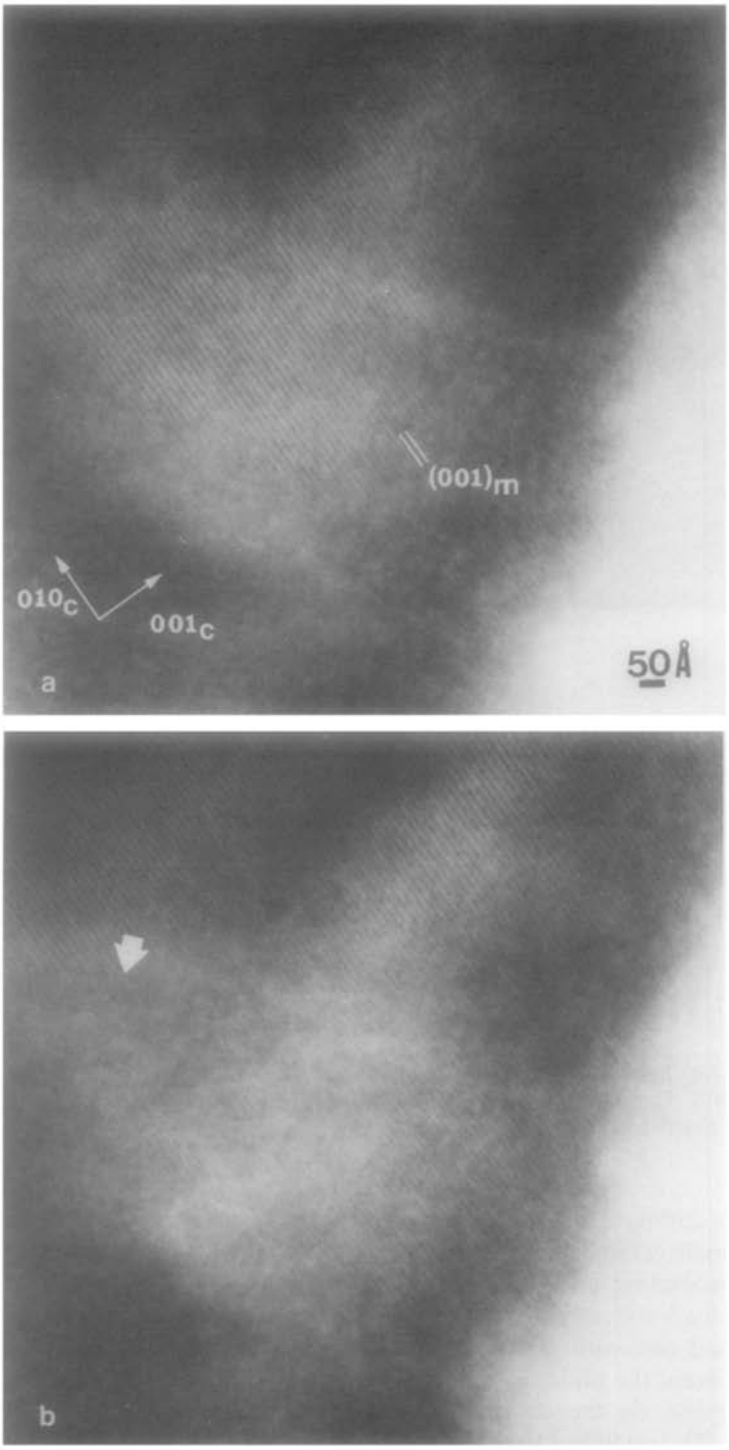

FIG. 4. A series of lattice images (from (a) to (d)) showing the transition from the low-temperature phase to the high-temperature phase. The beam direction is parallel to the $[100]_c$ axis.

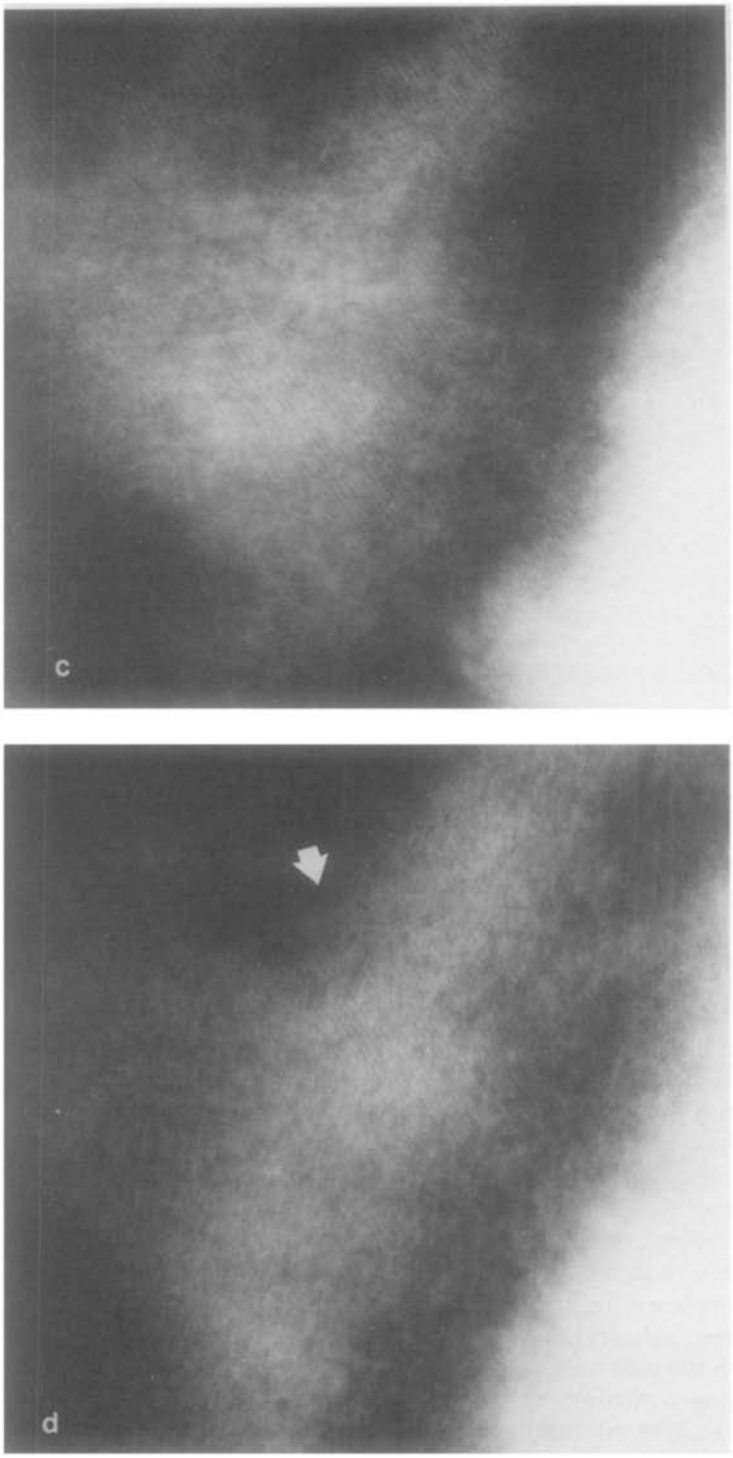

FIG. 4—*Continued.*

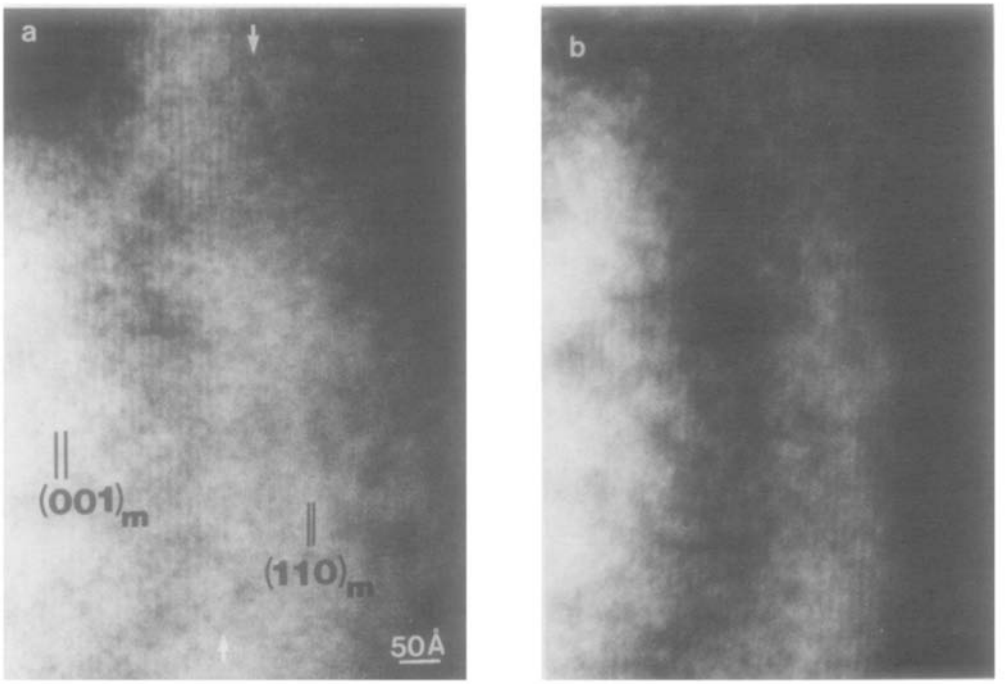

FIG. 5. A motion of a domain boundary in the low-temperature phase. In (a), the existence of a domain boundary is indicated by an arrow. The image (b) shows the same area after the domain boundary has moved toward left resulting in the rearrangement of the ordered structure in the domain on the left side.

cated by an arrow). In the domain on the left side of the boundary, the $[001]_m$ axis is parallel to the image plane; correspondingly, $(001)_m$ lattice fringes with the spacing of 16 Å are observed. On the other hand, in the domain on the right side, the $[001]_m$ axis is normal to the image plane and $(110)_m$ lattice fringes with the spacing of 8 Å are observed. The image in Fig. 5b was recorded immediately after the image in Fig. 5a (an interval of about 5 sec) had been taken. In Fig. 5b, the entire area shows the $(001)_m$ lattice fringes as a result of the motion of the domain boundary toward the right side of the area. This indicates that electrons in the domain on the right side of Fig. 5a had quickly rearranged themselves from one ordered orientation to another. (This is the first, direct observation of the motion of domain boundaries (*c* domains) of the low-temperature phase of Fe_3O_4 on the microscopic scale.) The motion of domain boundaries creates the change in magnetization, and at the same time, is accompanied by the relaxation of distortions; based on this observation of the domain boundary, this relaxation process seems to be related to magnetic after-effects observed in this phase (*36*).

Although the lattice images of the low-temperature phase observed in the present experiment are believed to be those due to the ordering of Fe^{2+} and Fe^{3+} ions, this observation still does not constitute a direct observation of the charge ordering for reasons given below. Therefore, controversies with respect to the symmetry of the charge ordering between that determined by diffraction studies and that indicated by some physical measurements remain unsolved.

However, the HREM study offers still another possibility for determining the ordered arrangement of Fe^{2+} and Fe^{3+} ions. Electron scattering is known to be very sensitive to valence states of ions for small scattering angles in comparison to X-ray and neutron scattering (*37, 38*). (This relation, for example, has led to the determination of the ionicity of vanadium ions in V_6O_{11} and V_7O_{13} through the analysis of electron diffraction intensities based on the many beam dynamical theory (*40*).) In the case of Fe_3O_4 the scattering factors of Fe^{2+} and Fe^{3+} ions for electrons are 15.9 and 22.0 Å, respectively, at the scattering angle corresponding to the 110_m superstructure reflection, while those for X ray are 23.62 and 22.70 at the corresponding scattering angle (*39*). Under the kinematical diffraction condition, therefore, low index superstructure reflections in electron diffraction have appreciable intensities which arise predominantly through the difference in scattering factor between Fe^{2+} and Fe^{3+} ions. The contribution of atomic diplacements, on the other hand, becomes significant for higher index reflections. This indicates the possibility of obtaining direct information on the charge ordering from lattice images taken from extremely thin areas where the dynamical effect does not play a significant role. In the present case, lattice images of the low-temperature phase have been obtained only from relatively thick areas. In such a case, because of strong dynamical effects, the contrast of lattice fringes corresponding to the low index superstructure reflections are significantly affected by higher index reflections whose amplitudes are predominantly contributed by atomic displacements. Therefore, these lattice images from thick areas cannot provide direct information on the ordered arrangement of Fe^{2+} and Fe^{3+} ions. The observation of lattice images of the low-temperature phase in this study, however, clearly indicates the feasibility of the approach described above.

Acknowledgments

The authors acknowledge their sincere thanks to Professor J. M. Honig for his valuable discussions. This work was supported by the National Science Foundation, MRL program, under Grant DMR-80-20249 and later by NSF Grant 8304314. Equipment provided through NSF Grant DMR-78-09025 was crucial to the success of this work.

References

1. R. W. Millar, *J. Amer. Chem. Soc.* **51,** 215 (1929).
2. T. Okamura, *Sci. Rep. Tohokn Imp. Univ.* **21,** 231 (1932).
3. E. J. Verway and P. W. Haayman, *Physica* **8,** 979 (1941).
4. T. Yamada, K. Suzuki, and S. Chikazumi, *Appl. Phys. Lett.* **13,** 172 (1968).
5. E. J. Samuelsen, E. J. Bleeker, L. Dobrzynski, and T. Riste, *J. Appl. Phys.* **39,** 114 (1968).
6. J. Yoshida and S. Iida, *J. Phys. Soc. Jpn.* **42,** 230 (1977).
7. J. Yoshida and S. Iida, *J. Phys. Soc. Jpn.* **47,** 1627 (1979).
8. G. T. Rado and J. M. Ferrari, *Phys. Rev. B* **12,** 5166 (1975).
9. G. T. Rado and J. M. Ferrari, *Phys. Rev. B* **15,** 290 (1977).
10. K. Shiratori, E. Kita, G. Kaji, A. Tasaki, S. Kimura, I. Shindo, and K. Kohn, *J. Phys. Soc. Jpn.* **47,** 1779 (1979).
11. G. Shirane, S. Chikazumi, J. Akimitsu, K. Chiba, M. Matsui, and Y. Fujii, *J. Phys. Soc. Jpn.* **39,** 949 (1975).
12. M. Iizumi and G. Shirane, *Solid State Commun.* **17,** 433 (1975).
13. M. Iizumi, T. F. Koetzle, G. Shirane, S. Chikazumi, M. Matsui, and S. Todo, *Acta Crystallogr. Sect. B* **38,** 2121 (1982).
14. R. S. Hargrove and W. Kündig, *Solid State Commun.* **13,** 1345 (1973).
15. M. Rubinstein and D. W. Forster, *Solid State Commun.* **9,** 1675 (1971).
16. B. J. Evans and E. F. Westrum, *Phys. Rev. B* **5,** 3791 (1972).
17. J. Maeda and S. Iida, *J. Phys. Soc. Jpn.* **39,** 1627 (1977).

18. J. MAEDA AND S. IIDA, *J. Phys. Soc. Jpn.* **42,** 1184 (1977).
19. S. UMEMURA AND S. IIDA, *J. Phys. Soc. Jpn.* **47,** 458 (1978).
20. E. L. BOYD, *Phys. Rev.* **129,** 1961 (1963).
21. N. M. KOVTUM AND A. A. SHAMYAKOV, *Solid State Commun.* **13,** 1345 (1973).
22. M. MIZOGUCHI, *J. Phys. Soc. Jpn.* **44,** 1501 (1978).
23. M. MIZOGUCHI, *J. Phys. Soc. Jpn.* **44,** 1512 (1978).
24. J. R. CULLEN, *Philos. Mag. B* **42,** 387 (1980).
25. S. IIDA, *Philos. Mag. B* **42,** 349 (1980).
26. J. C. H. SPENCE, "Experimental High Resolution Electron Microscopy," Oxford Univ. Press (Clarendon), Oxford (1980).
27. H. R. HARRISON AND R. ARAGON, *Mater. Res. Bull.* **13,** 1097 (1978).
28. H. R. HARRISON, R. ARAGON, J. E. KEAM, AND J. M. HONIG, "Inorganic Synthesis" (S. L. Holt, Ed.), Vol. 22, p. 43, Wiley, New York (1983).
29. R. ARAGON, D. J. BUTTEREY, J. P. SHEPHERD, AND J. M. HONIG, *Phys. Rev. B,* in press.
30. J. P. SHEPHERD, J. W. ROENDTZER, R. ARAGON, C. J. S. SANDBERG, AND J. M. HONIG, *Phys. Rev. B,* in press.
31. M. O. RIGO AND J. KLEINCLAUSS, *Philos. Mag. B* **42,** 393 (1980).
32. E. J. VERWEY, P. W. HAAYMAN, AND F. C. ROMEIJAN, *J. Chem. Phys.* **15,** 181 (1947).
33. N. F. MOTT, Festkörperproblem, XIX (Vieweg, Braunschweig), 331 (1979).
34. E. CALLEN, *Phys. Rev.* **150,** 367 (1966).
35. M. MATSUI, S. TODO, AND C. CHIKAZUMI, *J. Phys. Soc. Jpn.* **43,** 47 (1977).
36. H. KRONMÜLLER AND F. WALZ, *Philos. Mag. B* **42,** 433 (1980).
37. B. K. VAINSHTEIN, "Structure Analysis by Electron Diffraction," Pergamon, Oxford (1969).
38. S. NAGAKURA, *J. Phys. Soc. Jpn.* **25,** 488 (1968).
39. "International Tables for X-Ray Crystallography," Vol. III, 2nd ed., Kynoch Press, Birmingham (1968).
40. Y. HIROTSU, H. SATO, AND S. NAGAKURA, *in* "AIP Conference Proceedings," No. 53; "Modulated Structures, 1979;" (J. B. Cohen, M. B. Solamon, and B. J. Buensch, Eds.), p. 75, American Institute of Physics (1979).